

REPORT No. 880

ANALYSIS OF JET-PROPULSION-ENGINE COMBUSTION-CHAMBER PRESSURE LOSSES

By I. IRVING PINKEL and HAROLD SHAMES

SUMMARY

The development and the use of a chart for estimating the pressure losses in jet-engine combustion chambers are described. By means of the chart, the pressure losses due to fluid friction and to momentum changes in the air flow accompanying combustion can be separately evaluated.

The pressure-loss chart is based on the assumption that the pressure losses in the actual combustion chamber can be matched by those of an equivalent combustion chamber of constant cross-sectional area. The concept of the equivalent combustion chamber serves as a convenient basis for comparing the pressure-loss characteristics of combustion chambers of a variety of designs. By means of the chart, the pressure losses of a combustion chamber can be specified by two numbers, one related to the friction pressure-loss characteristics and the other to the momentum pressure-loss characteristics of the combustion chamber.

The over-all pressure losses computed from the pressure-loss chart are within 7 percent of the experimental values for the three types of combustion chamber considered herein.

INTRODUCTION

The jet-propulsion engine, in common with other internal-combustion engines, utilizes fuel-air mixtures as the working substance in the engine cycle. For this reason, the manner of heat addition to the working substance and the flow characteristics of the combustion chamber have a marked effect on the performance of the jet-propulsion engine. In particular, combustion-chamber pressure losses result in reduced cycle efficiency and lowered mass air flow through the engine with a consequent reduction in engine thrust.

A chart was developed at the NACA Cleveland laboratory in 1945 to estimate combustion-chamber pressure losses in which the pressure losses due to fluid friction and the losses due to the addition of heat by combustion are separately evaluated. The pressures considered are total or stagnation pressures unless otherwise specified. Pressure losses obtained with the chart are compared with the losses experimentally obtained for three current types of jet-propulsion-engine combustion chamber.

DESCRIPTION OF SOME CURRENT TYPES OF COMBUSTION CHAMBER FOR JET-PROPULSION ENGINES

A cylindrical type of combustion chamber used in turbojet engines is shown in figure 1 (a). The outside cylinder

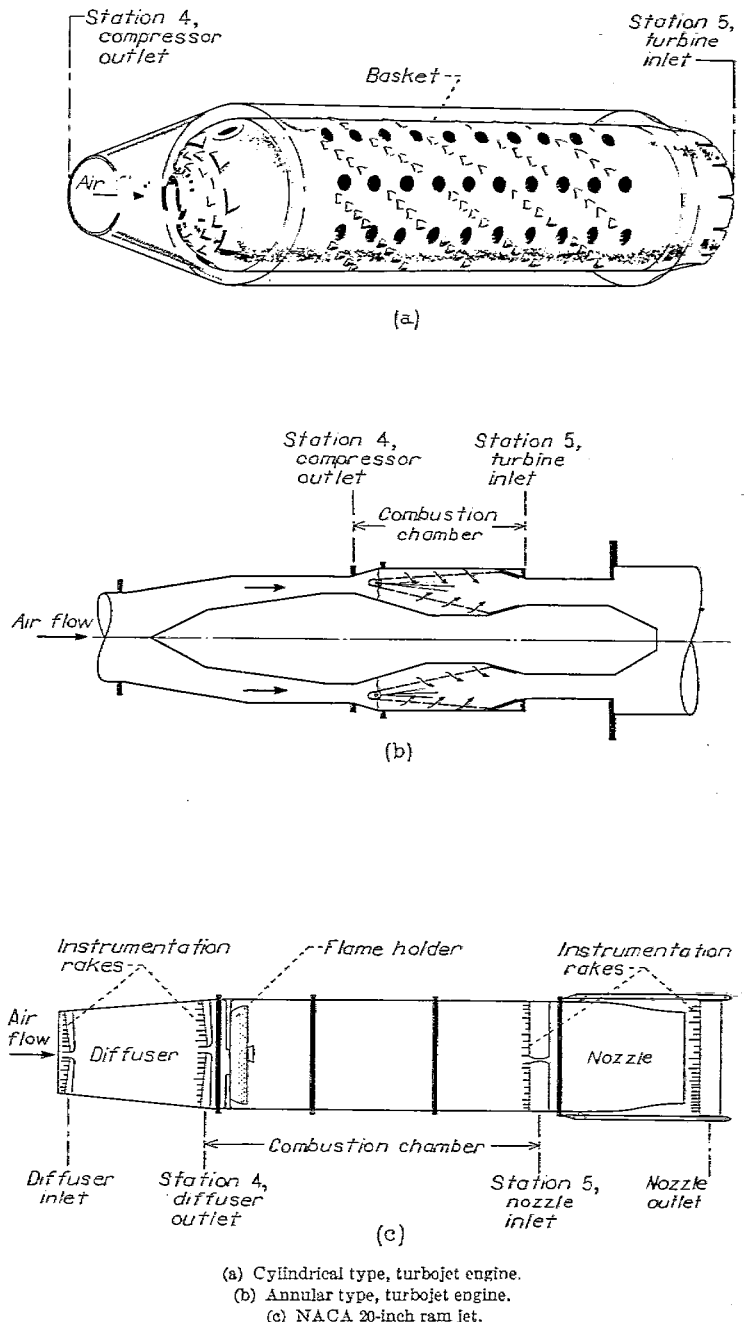


FIGURE 1.—Schematic views of various combustion chambers for jet-propulsion engines.

and the entrance section form a duct to carry the air from the compressor outlet to the turbine inlet. The inside cylinder, referred to as the "basket," surrounds the com-

bustion zone. The basket is fitted with a dome having entrance slots for inducting part of the total air flow into the combustion chamber in such a manner as to provide good mixing with the fuel injected inside the dome. As combustion proceeds, the remainder of the air enters the combustion zone through holes arranged along the cylindrical surface of the basket. In this manner, the flow is split into primary and secondary streams to obtain fuel-air ratios in the combustion zone closer to stoichiometric than would be provided by mixing the fuel with the total air flow. The combustion rate and the ignition characteristics are thereby improved and the walls of the basket are cooled by the secondary air. This type of combustion chamber is usually installed in multiple units arranged in parallel.

The annular type of combustion chamber used in turbojet engines is shown in figure 1 (b). The combustion-chamber annulus is formed by inside and outside walls that are coaxial with the drive shaft connecting the turbine and the compressor. This annular duct carries the total air flow from the compressor outlet to the turbine inlet. The toroidal basket is approximately triangular in section and is provided with slots and holes for splitting the flow into primary and secondary streams.

A form of combustion chamber for the ram jet consists of a single cylindrical duct provided with a flame holder at the fuel-injection zone (fig. 1 (c)). The combustion zone extends downstream of the flame holder. No basket is used in the ram jet in order to avoid the pressure losses involved in getting the air flow through the holes in a basket.

The three types of combustion chamber considered have in common an obstruction interposed between the combustion-chamber inlet and the combustion zone. This obstruction to the air flow, which may be either a flame holder or a basket, causes a loss in total pressure between the combustion-chamber inlet and the combustion zone. The combustion zone is unobstructed in these three types of combustion chamber. No combustion chambers with structures in the combustion zone, such as fuel preheaters and vaporizers, catalytic surfaces, and heating elements, are considered.

SYMBOLS

The symbols in this report conform with those currently used for turbojet engines. Symbols used more than once are listed here for ready reference.

A	area of cross section of equivalent combustion chamber of constant cross section, square feet
C	constant
g	factor for converting slugs to pounds mass, 32.2
K	combustion-chamber pressure-loss factor
M	Mach number, ratio of airspeed to local speed of sound
N	engine rotational speed, rpm
P	total (stagnation) pressure, pounds per square foot absolute
ΔP_F	loss in total pressure due to friction (friction pressure loss), pounds per square foot
ΔP_M	loss in total pressure due to heat addition to air flow by combustion (momentum pressure loss), pounds per square foot

ΔP_T	over-all loss in total pressure due to friction and heat addition, pounds per square foot
p	static pressure, pounds per square foot absolute
R	gas constant for air, 53.3 foot-pounds per pound per °R
T	total (stagnation) temperature, °R
t	static temperature, °R
v	speed of gas flow, feet per second
\dot{W}	air mass flow, pounds per second
γ	ratio of specific heat at constant pressure to specific heat at constant volume
η_c	compressor efficiency
θ_2	ratio of total temperature of compressor-inlet air to static temperature of standard NACA air at sea level
ρ	air density, pounds per cubic foot
ρ_T	air density measured under total (stagnation) conditions, pounds per cubic foot
Subscripts:	
2	compressor inlet
4	combustion-chamber inlet, also compressor outlet of turbojet engine or diffuser outlet of ram jet
5	combustion-chamber outlet, also turbine inlet of turbojet engine or nozzle inlet of ram jet
B	entrance to combustion zone of equivalent combustion chamber

DEVELOPMENT OF PRESSURE-LOSS CHART

Assumption.—The development of the combustion-chamber pressure-loss chart is based on the assumption that the pressure-loss characteristics of the actual combustion chamber can be matched by those of an equivalent combustion chamber of constant cross-sectional area having the form shown in figure 2. The air enters the combustion chamber from the left and experiences a loss in total pressure due to friction in the zone from station 4 to station B . This friction pressure loss ΔP_F corresponds to the pressure loss in the actual combustion chamber involved in bringing both the primary and secondary air from the compressor outlet, or the diffuser outlet for the ram jet, through the basket, or the flame holder, into the combustion zone. This loss is the pressure loss measured across the actual combustion chamber with the air flowing but no combustion taking place. All the pressure loss due to friction is assumed to occur before the air becomes involved in the combustion. The losses in the combustion-chamber-inlet section and those involved in getting the air through the basket, or the flame holder, are considered to account for most of the fluid-friction pressure

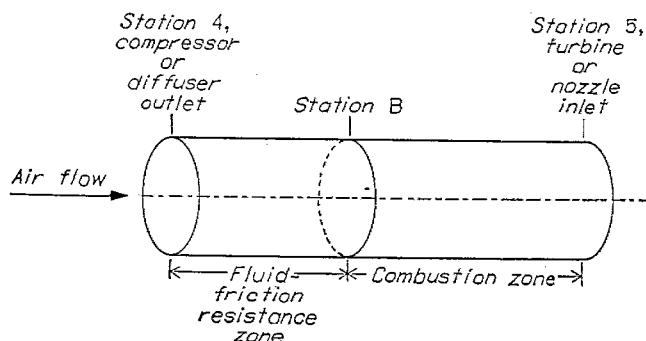


FIGURE 2.—Equivalent combustion chamber of constant cross-sectional area.

losses in the combustion chamber. The use of the pressure-loss chart is therefore restricted to combustion chambers having an unobstructed combustion zone. Pressure losses, designated momentum pressure losses ΔP_M , also occur in the combustion zone with the addition of heat to the flowing gas. The over-all loss in total pressure ΔP_T in the combustion chamber is the sum of the friction and momentum pressure losses:

$$\Delta P_T = \Delta P_F + \Delta P_M \quad (1)$$

No account is taken of the effect of fuel injection on the mass flow and the gas velocity through the combustion zone. For the turbojet engine, in which the fuel-air ratio is low because of the temperature limitation imposed by the turbine material, the error involved in neglecting the fuel addition in the expression for the computed combustion-chamber pressure losses is small.

Theoretical consideration.—The theoretical considerations involved in developing the combustion-chamber pressure-loss chart use the equivalent combustion chamber of constant cross-sectional area (fig. 2) as the model. The analysis is made in three steps: An expression is obtained for the friction pressure loss in terms of the combustion-chamber inlet-air conditions. The conditions at the entrance to the combustion zone are evaluated to account for the effect of friction pressure loss on the air flow. The equations required for computing the momentum pressure loss are then obtained, based on the combustion-zone entrance conditions and the total temperature ratio across the combustion chamber.

General laws for fluid-friction pressure losses indicate the following relation among ΔP_F , W , and ρ_T :

$$\Delta P_F = \frac{KW^2}{\rho_T A} = \frac{KW^2 R T_4}{P_4} \quad (2)$$

Equation (2) is in agreement with experimental data obtained with the combustion chambers of the turbojet engine and the ram jet. For convenience in setting up the pressure-loss chart, the friction pressure loss is related to the Mach number of flow at the entrance to the equivalent combustion chamber. From the expression for the Mach number

$$M^2 = \frac{v^2}{\gamma g R t}$$

and the relation satisfying the law of conservation of mass for steady flow in the combustion chamber

$$W = \rho A v$$

the following equation is obtained:

$$M^2 = \frac{\rho^2 A^2 v^2 (Rt)}{\gamma g A^2 (\rho R t)^2} = \frac{W^2 R t}{\gamma g A^2 P^2} = \frac{W^2 R T}{\gamma g A^2 P^2} \left(1 + \frac{\gamma - 1}{2} M^2\right)^{\frac{\gamma + 1}{\gamma - 1}} \quad (3)$$

In the derivation of equation (3), use is made of the perfect gas law and the reversible adiabatic relations

$$\frac{T}{t} = 1 + \frac{\gamma - 1}{2} M^2$$

and

$$\frac{P}{p} = \left(\frac{T}{t}\right)^{\frac{\gamma}{\gamma - 1}}$$

Equations (2) and (3) applied to station 4 yield the desired relation

$$\frac{\Delta P_F}{P_4} = \frac{KW^2 R T_4}{P_4^2} = \frac{\gamma_4 g K A^2 M_4^2}{\left(1 + \frac{\gamma_4 - 1}{2} M_4^2\right)^{\frac{\gamma_4 + 1}{\gamma_4 - 1}}} \quad (4)$$

The second term in equation (4) $\frac{KW^2 R T_4}{P_4^2}$ shows that the friction pressure-loss ratio $\Delta P_F/P_4$ depends only on the air mass flow and the total temperature and pressure at the entrance to the combustion chamber. No choice of the cross-sectional area A of the equivalent combustion chamber need be made at this stage of development but a value will later be chosen to give the correct value of ΔP_M .

The Mach number of the flow at the entrance to the combustion zone M_B differs from the Mach number of the combustion-chamber inlet M_4 because of the friction pressure loss experienced by the flow. The expression relating these quantities is obtained by means of equation (3), as applied to stations 4 and B . Inasmuch as the total temperature of the gases at stations 4 and B are the same

$$W \sqrt{T_4} = W \sqrt{T_B} = \frac{\sqrt{\frac{\gamma_4 g}{R}} A M_4 P_4}{\left(1 + \frac{\gamma_4 - 1}{2} M_4^2\right)^{\frac{\gamma_4 + 1}{2(\gamma_4 - 1)}}} = \frac{\sqrt{\frac{\gamma_B g}{R}} A M_B P_B}{\left(1 + \frac{\gamma_B - 1}{2} M_B^2\right)^{\frac{\gamma_B + 1}{2(\gamma_B - 1)}}}$$

The value of γ_4 may be assumed equal to γ_B because t_4 is not appreciably different from t_B . The equation used to correct M_4 to M_B is

$$1 - \frac{P_B}{P_4} = \frac{P_4 - P_B}{P_4} = \frac{\Delta P_F}{P_4} = 1 - \frac{M_4}{M_B} \left(\frac{1 + \frac{\gamma_4 - 1}{2} M_B^2}{1 + \frac{\gamma_4 - 1}{2} M_4^2} \right)^{\frac{\gamma_4 + 1}{2(\gamma_4 - 1)}} \quad (5)$$

The following expression for momentum pressure-loss ratio $\Delta P_M/P_B$ for an unobstructed combustion chamber of uniform cross-sectional area is developed in the appendix:

$$\frac{\Delta P_M}{P_B} = 1 - \frac{(1 + \gamma_B M_B^2) \left(1 + \frac{\gamma_5 - 1}{2} M_5^2\right)^{\frac{\gamma_5}{\gamma_5 - 1}}}{(1 + \gamma_5 M_5^2) \left(1 + \frac{\gamma_B - 1}{2} M_B^2\right)^{\frac{\gamma_B}{\gamma_B - 1}}} \quad (6)$$

In order to use equation (6), a relation among M_5 , the known value of M_B , and the temperature ratio across the combustion chamber T_5/T_4 is required. This relation is obtained by writing equation (3) as applied to stations B and 5 successively

$$\frac{W^2 T_B}{P_B^2} = \frac{\frac{\gamma_B g}{R} A^2 M_B^2}{\left(1 + \frac{\gamma_B - 1}{2} M_B^2\right)^{\frac{\gamma_B + 1}{\gamma_B - 1}}}$$

$$\frac{W^2 T_5}{P_5^2} = \frac{\frac{\gamma_5 g}{R} A^2 M_5^2}{\left(1 + \frac{\gamma_5 - 1}{2} M_5^2\right)^{\frac{\gamma_5 + 1}{\gamma_5 - 1}}}$$

By division of these equations and from the fact that the total temperatures at the combustion-chamber inlet and at

the entrance to the combustion zone are equal, that is, $T_4 = T_B$, there is obtained

$$\frac{T_5}{T_4} \left(\frac{P_B}{P_5} \right)^2 = \frac{\gamma_5 M_5^2 \left(1 + \frac{\gamma_B - 1}{2} M_B^2 \right)^{\frac{\gamma_B + 1}{\gamma_B - 1}}}{\gamma_B M_B^2 \left(1 + \frac{\gamma_5 - 1}{2} M_5^2 \right)^{\frac{\gamma_5 + 1}{\gamma_5 - 1}}}$$

The term $(P_B/P_5)^2$ is eliminated from this expression by applying the reciprocal of equation (14) in the appendix,

$$\frac{P_B}{P_5} = \frac{(1 + \gamma_5 M_5^2) \left(1 + \frac{\gamma_B - 1}{2} M_B^2 \right)^{\frac{\gamma_B}{\gamma_B - 1}}}{(1 + \gamma_B M_B^2) \left(1 + \frac{\gamma_5 - 1}{2} M_5^2 \right)^{\frac{\gamma_5}{\gamma_5 - 1}}}$$

The final expression is

$$\frac{T_5}{T_4} = \frac{\gamma_5 M_5^2 (1 + \gamma_B M_B^2)^2 \left(1 + \frac{\gamma_5 - 1}{2} M_5^2 \right)}{\gamma_B M_B^2 (1 + \gamma_5 M_5^2)^2 \left(1 + \frac{\gamma_B - 1}{2} M_B^2 \right)} \quad (7)$$

Equations (6) and (7) are used to compute $\Delta P_M/P_B$ from the known values of M_B and the temperature ratio T_5/T_4 .

Construction of pressure-loss chart.—From the pressure-loss chart shown in figure 3, ΔP_F , ΔP_M , and ΔP_T can be obtained from known values of the combustion-chamber-inlet parameter $W\sqrt{T_4}/P_4$ and the temperature ratio across the combustion chamber. The chart is set up in the following manner: Quadrant IV gives a plot of $W\sqrt{T_4}/P_4$ against M_4 according to equation (3), modified as

$$\frac{W\sqrt{T_4}}{P_4} = \frac{\sqrt{\frac{\gamma_4 g}{R}} A M_4}{\left(1 + \frac{\gamma_4 - 1}{2} M_4^2 \right)^{\frac{\gamma_4 + 1}{2(\gamma_4 - 1)}}}$$

for several values of the parameter A . The variation of $\Delta P_F/P_4$ with M_4 according to equation (4) is given in quadrant I for several values of the parameter KA^2 , where K is defined by equation (2). The curves in quadrant II correct M_4 to M_B to account for the change in Mach number accompanying the friction pressure loss ΔP_F . This correction is made by means of equation (5). In quadrant II, $\Delta P_F/P_4$ is plotted against M_B for various values of M_4 . In quadrant III, $\Delta P_M/P_B$ is plotted against M_B according to equations (6) and (7) for various values of the temperature ratio T_5/T_4 . The values of γ_5 used in equations (6) and (7) to obtain the curves of quadrant III are average values for the temperature range corresponding to the temperature ratio T_5/T_4 and the required fuel-air ratio with an assumed 95-percent combustion efficiency. In order to obtain the temperature range, it was assumed that T_4 was 600° R for values of T_5/T_4 less than 3.8

and 400° R for T_5/T_4 values greater than 3.8. These values of T_4 approximate those of the turbojet engine and ram jet, respectively. The over-all pressure-loss ratio $\Delta P_T/P_4$ is obtained from the values of $\Delta P_F/P_4$ and $\Delta P_M/P_B$ given by the chart by means of the expression

$$\frac{\Delta P_T}{P_4} = \left(\frac{\Delta P_F}{P_4} + \frac{\Delta P_M}{P_B} \right) \left(1 - \frac{\Delta P_F}{P_4} \right) + \left(\frac{\Delta P_F}{P_4} \right)^2 \quad (8)$$

derived from equation (1) and the relation

$$P_B = P_4 - \Delta P_F$$

For most applications of the chart, little error is made if P_B is assumed equal to P_4 in the denominator of the pressure-loss-ratio terms and equation (8) is expressed simply as

$$\frac{\Delta P_T}{P_4} = \frac{\Delta P_F}{P_4} + \frac{\Delta P_M}{P_4} \approx \frac{\Delta P_F}{P_4} + \frac{\Delta P_M}{P_B} \quad (8a)$$

USE OF PRESSURE-LOSS CHART

The chart is used in the following manner to obtain the various pressure losses: Assume, temporarily, that the value of K is 1.0 and A is 0.20 square foot for the combustion chamber. For a known value of $W\sqrt{T_4}/P_4$ equal to 0.0230 and the temperature ratio T_5/T_4 of 3.40, the pressure losses due to friction and momentum are evaluated in four steps around the chart. Start with the known value of $W\sqrt{T_4}/P_4$ on the ordinate of quadrant IV. From the curve having the value of A equal to 0.20, M_4 is determined to be 0.126 on the abscissa of quadrant IV and the corresponding value of 0.0278 for $\Delta P_F/P_4$ is obtained by means of the curve in quadrant I having the value of 0.04 for KA^2 for the combustion chamber. Proceed parallel to the abscissa through this value of $\Delta P_F/P_4$ to the curve in quadrant II having the value of M_4 previously established; the value of 0.130 for M_B is determined on the abscissa of quadrant II. From the T_5/T_4 curve having the value of 3.40 in quadrant III, $\Delta P_M/P_B$ is determined to be 0.0276 on the ordinate of quadrant III. The over-all pressure-loss ratio $\Delta P_T/P_4$ is then computed to be 0.0554 by adding $\Delta P_M/P_B$ to $\Delta P_F/P_4$.

Determination of K and A .—The values of K and A for a given combustion chamber can be determined by means of the pressure-loss chart if $\Delta P_T/P_4$ and $\Delta P_F/P_4$ are known from experiment for the same value of $W\sqrt{T_4}/P_4$. The pressure loss due to friction ΔP_F is measured by total-pressure tubes located at the combustion-chamber inlet and outlet with air flowing through the combustion chamber without combustion taking place. The over-all pressure loss is obtained with these pressure tubes with the air flowing at the same value of $W\sqrt{T_4}/P_4$ and combustion taking place at a known value of T_5/T_4 . In figure 4, an enlarged section of figure 3, a construction is demonstrated in which the values of A and KA^2 were established for a cylindrical-type combustion cham-

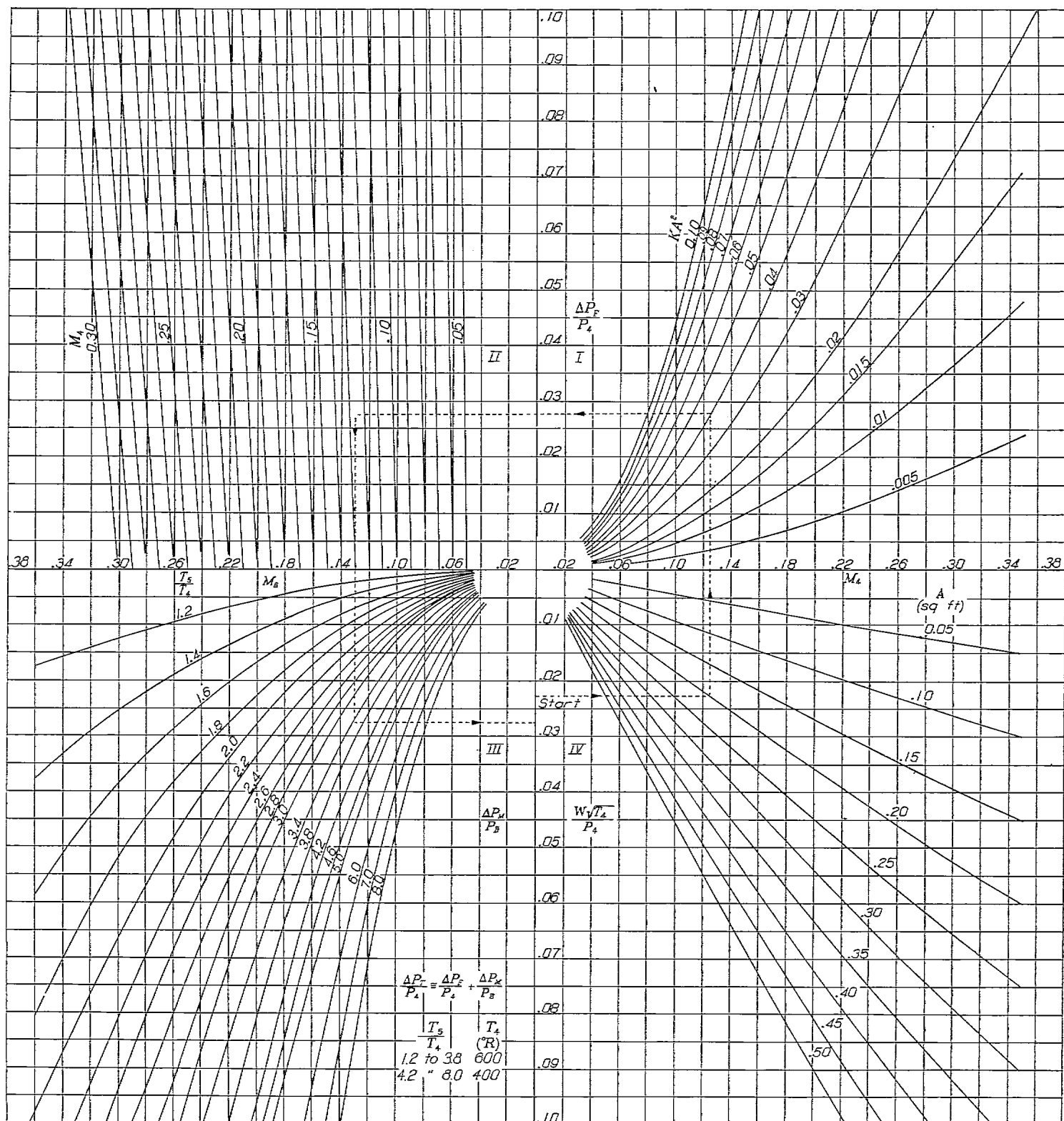


FIGURE 3.—Combustion chamber pressure-loss chart. (A large copy of this chart can be obtained upon request from the NACA.)

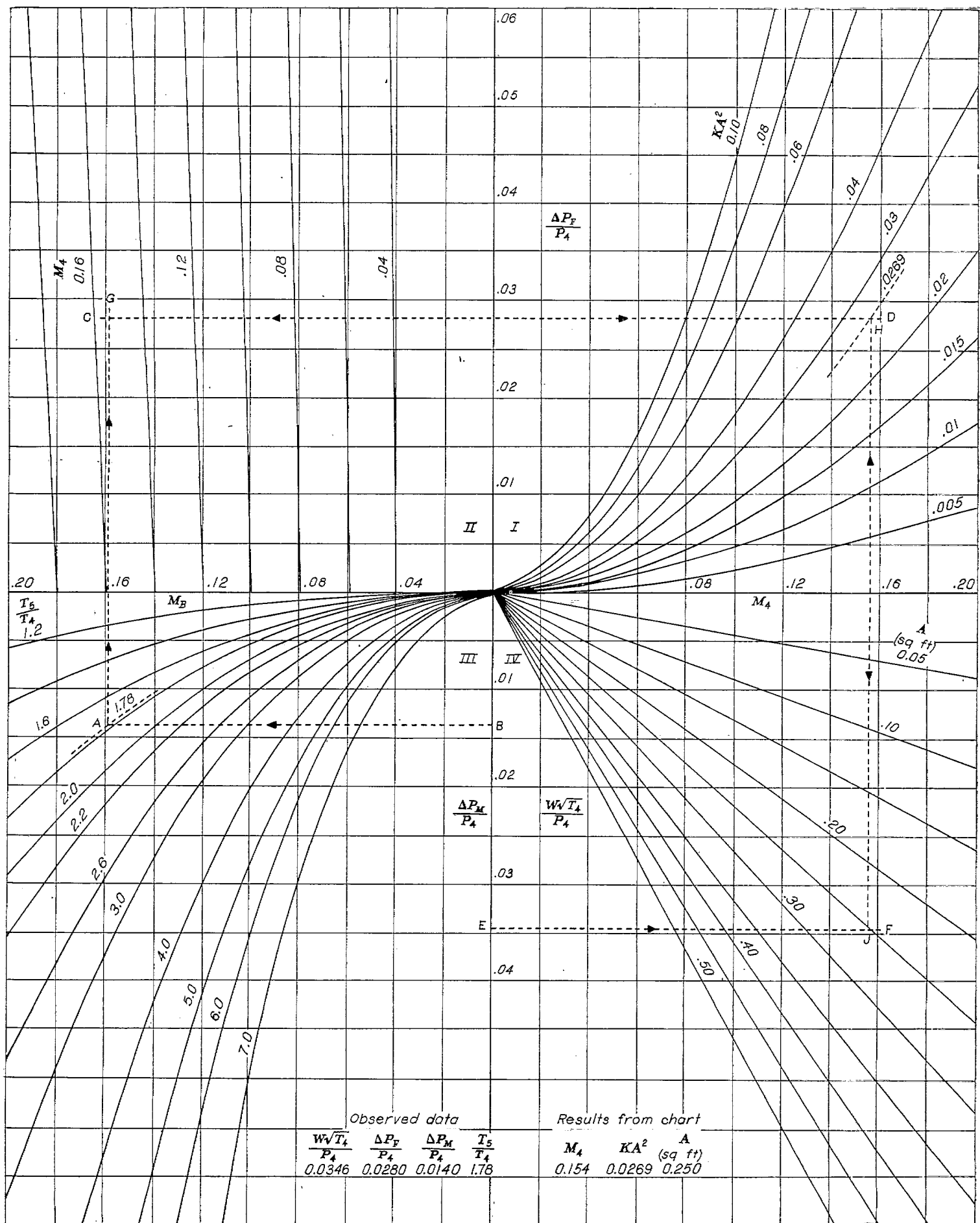
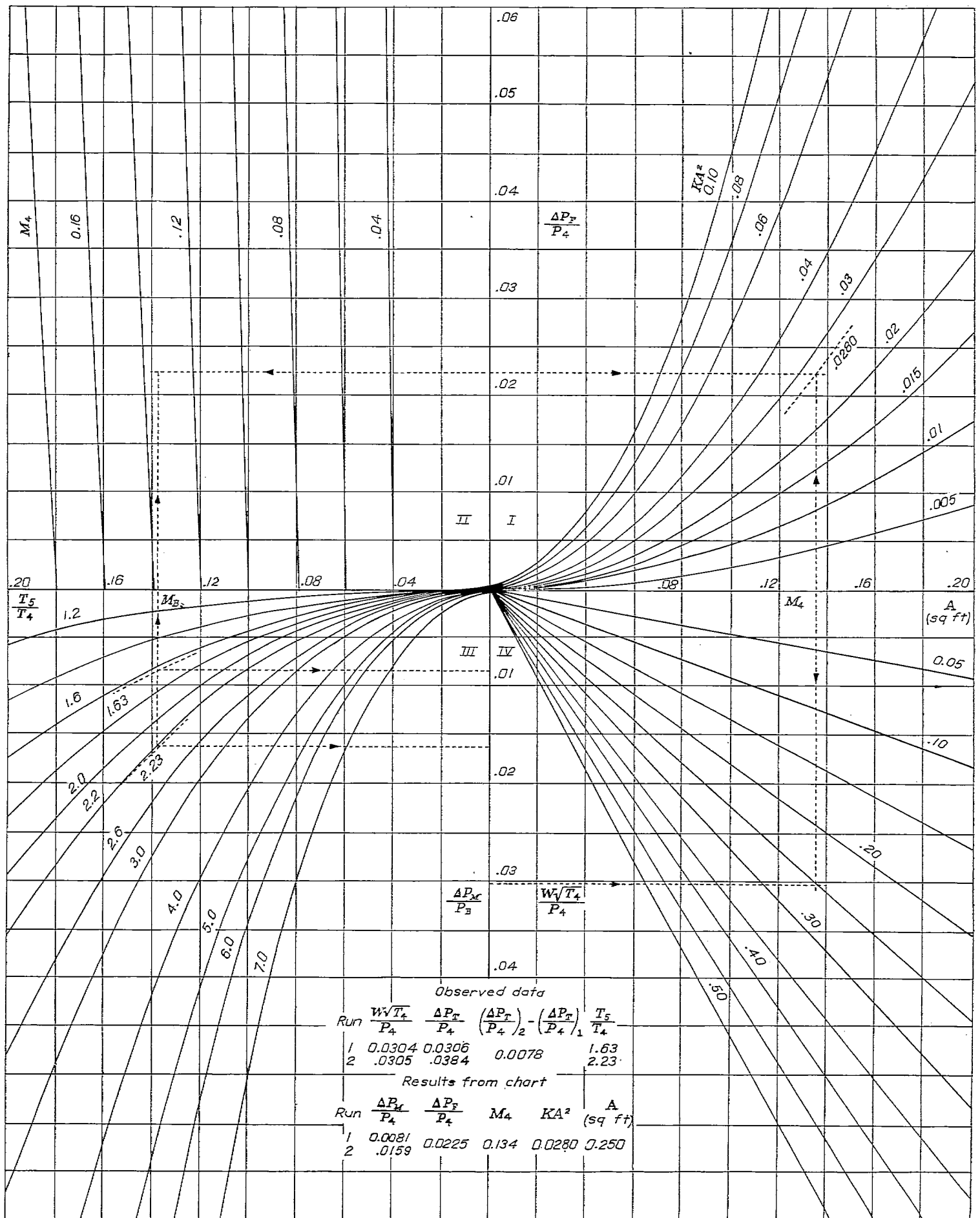


FIGURE 4.—Determination of KA^2 and A from measured values of ΔP_F and ΔP_r .

FIGURE 5.—Determination of KA^2 and A from two measured values of ΔP_T .

ber by means of the following experimentally determined data:

$$\frac{W\sqrt{T_4}}{P_4}=0.0346$$

$$\frac{\Delta P_T}{P_4}=0.0420$$

$$\frac{\Delta P_F}{P_4}=0.0280 \text{ (from engine windmilling data)}$$

$$\frac{\Delta P_M}{P_B}=\frac{\Delta P_T}{P_4}-\frac{\Delta P_F}{P_4}=0.0140 \text{ (according to equation (8a))}$$

$$\frac{T_5}{T_4}=1.78$$

Line BA, quadrant III, was drawn parallel to the abscissa through the known value of $\Delta P_M/P_B$ and ends on the proper T_5/T_4 curve. Line CD was drawn parallel to the abscissa through the value of $\Delta P_F/P_4$; line EF was drawn parallel to the abscissa through the value of $W\sqrt{T_4}/P_4$; line AG was drawn parallel to the ordinate. The intersection of lines AG and CD determined a value of M_4 . The line HJ was taken parallel to the ordinate through M_4 on the abscissa of quadrant I. The intersection of line HJ with line CD determined the value of KA^2 for the cylindrical-type combustion chamber. The intersection of lines EF and HJ similarly determined the value of A in quadrant IV.

If ΔP_F is known for a different value of $W\sqrt{T_4}/P_4$ than corresponds to ΔP_T , the required value of ΔP_F corresponding to ΔP_T can be obtained by evaluating K in equation (2) with the known values of ΔP_F and corresponding value of $W\sqrt{T_4}/P_4$. The required value of ΔP_F may then be obtained by using this value of K and the value of $W\sqrt{T_4}/P_4$ corresponding to ΔP_T .

A method of obtaining KA^2 and A for a combustion chamber when only the over-all loss in total pressure ΔP_T can be obtained is shown in figure 5, also an enlarged section of figure 3. It is assumed that, for a known value of $W\sqrt{T_4}/P_4$, two values of $\Delta P_T/P_4$ can be measured which correspond to two different known values of the combustion-chamber temperature ratio T_5/T_4 . The value of $\Delta P_F/P_4$ is the same for both cases because $W\sqrt{T_4}/P_4$ is the same (equation (4)). The difference in the measured values of $\Delta P_T/P_4$ represents the difference in the values of $\Delta P_M/P_B$ (equation (8a)). This difference is set on a divider according to the scale of the ordinate of quadrant III (fig. 5). With the line joining the divider points held parallel to the ordinate, one leg of the divider is moved along one of the curves in quadrant III having one of the values of T_5/T_4 used in the tests until the other leg of the divider intercepts the curve having the other value of T_5/T_4 . The values of $\Delta P_M/P_B$ are thus determined for both engine conditions and the value of $\Delta P_F/P_4$ is obtained by subtracting $\Delta P_M/P_B$ from the corresponding value of $\Delta P_T/P_4$ (equation (8a)). A construction similar to that described in the previous paragraph can now be made to obtain A and KA^2 , as shown in figure 5 for the experimental data given in the insert.

Remarks concerning the use of the chart.—The values of $W\sqrt{T_4}/P_4$ for turbojet engines may be obtained from the compressor performance data. The operating line for a compressor is often given as a plot of the pressure ratio across the compressor P_4/P_2 against corrected engine speed $N\sqrt{\theta_2}$ and corrected air-weight flow $\frac{2116}{\sqrt{519}} W \frac{\sqrt{T_2}}{P_2}$. For each corrected engine speed there corresponds a value of P_4/P_2 and $W\sqrt{T_2}/P_2$ for a given flight speed and altitude. The factor $W\sqrt{T_4}/P_4$ is computed from these data by dividing $W\sqrt{T_2}/P_2$ by P_4/P_2 and evaluating T_4 from the relation

$$T_4=T_2\left[\frac{\left(\frac{P_4}{P_2}\right)^{\frac{\gamma-1}{\gamma}}-1}{\eta_c}+1\right]$$

where η_c is the compressor efficiency. The compressor efficiency is obtained from compressor performance data.

For combustion chambers having air-flow rates $W\sqrt{T_4}/P_4$ large enough to make the value of the entrance parameter $W\sqrt{T_4}/P_4$ exceed the limits on the chart, only a segment of the combustion chamber is considered. Assume, for example, that a 30° segment of the combustion chamber, which carried one-twelfth the total air flow, gives values of $W\sqrt{T_4}/P_4$ that fit the scale of the chart. The value of A is then one-twelfth that for the complete combustion chamber. The value of K is 144 times that for the complete combustion chamber (equation (2)). The value of KA^2 is the same for the segment and the complete combustion chamber. This property of the parameter KA^2 led to the choice of the pressure-loss chart arrangement given in figure 3, where KA^2 rather than K is taken as the parameter in quadrant I. The various pressure losses for the segment are the same as those of the complete

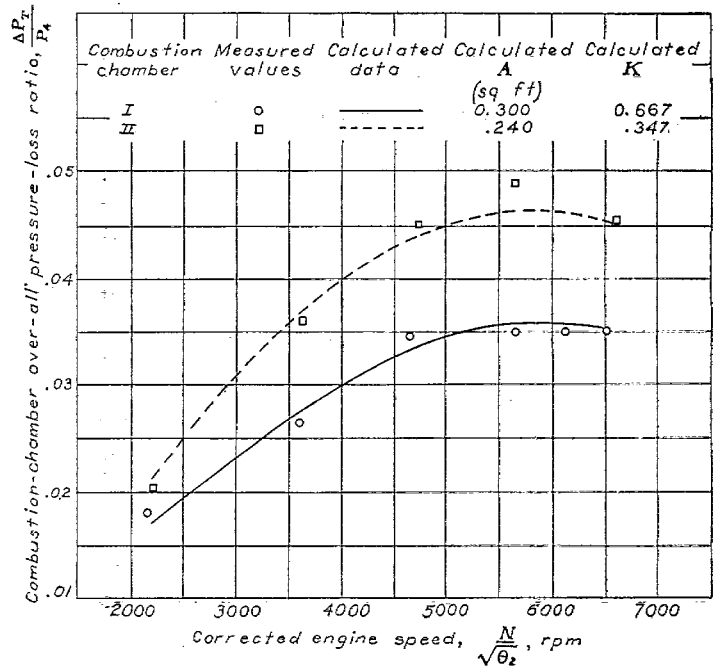


FIGURE 6.—Comparison of experimental and computed over-all pressure-loss ratios for two cylindrical-type combustion chambers.

combustion chamber. The construction for obtaining K and A for the segment is the same as that described for the complete combustion chamber. The values of pressure losses and temperature ratio obtained by experiment with the complete combustion chamber are used and the value of W corresponds to the air flow through the segment.

A variety of forms of the pressure-loss chart is possible. The form presented in figures 3 to 5 is considered to have the most general utility. For special application, several of the quadrants can be combined for ease of manipulation.

RESULTS AND DISCUSSION

Comparison of experimental and computed pressure losses.—A comparison of experimental with computed combustion-chamber pressure losses is given for the cylindrical, annular, and ram-jet types of combustion chamber illustrated in figure 1.

The data for the pressure losses of the cylindrical combustion chamber were obtained from tests of a complete jet-propulsion engine in the Cleveland altitude wind tunnel. Figure 6 shows experimental and computed over-all pressure-loss ratios for two cylindrical combustion chambers installed in the same engine. The maximum difference between the measured and calculated values is less than 6 percent. These combustion chambers differ only in the primary entrance arrangements on the dome of the basket and in the relative proportion of primary and secondary air. For combustion chamber I, A is computed to be 0.300 square foot and K is computed to be 0.667. For combustion chamber II, A is computed to be 0.240 square foot and K is computed to be 0.347. Type I has the higher value of K and therefore the higher values of friction pressure-loss ratio (fig 7 (a)); type II has the lower value of A and therefore the higher momentum pressure-loss ratio (fig. 7 (b)). The actual area of cross section of the combustion zone was approximately 0.29 square foot. These data serve to illustrate how the values of K and A are influenced by the relative proportions and manner of induction of primary and secondary air as well as the gross geometry of the combustion chamber.

Comparison of computed and experimental values of the pressure losses in an annular combustion chamber and a

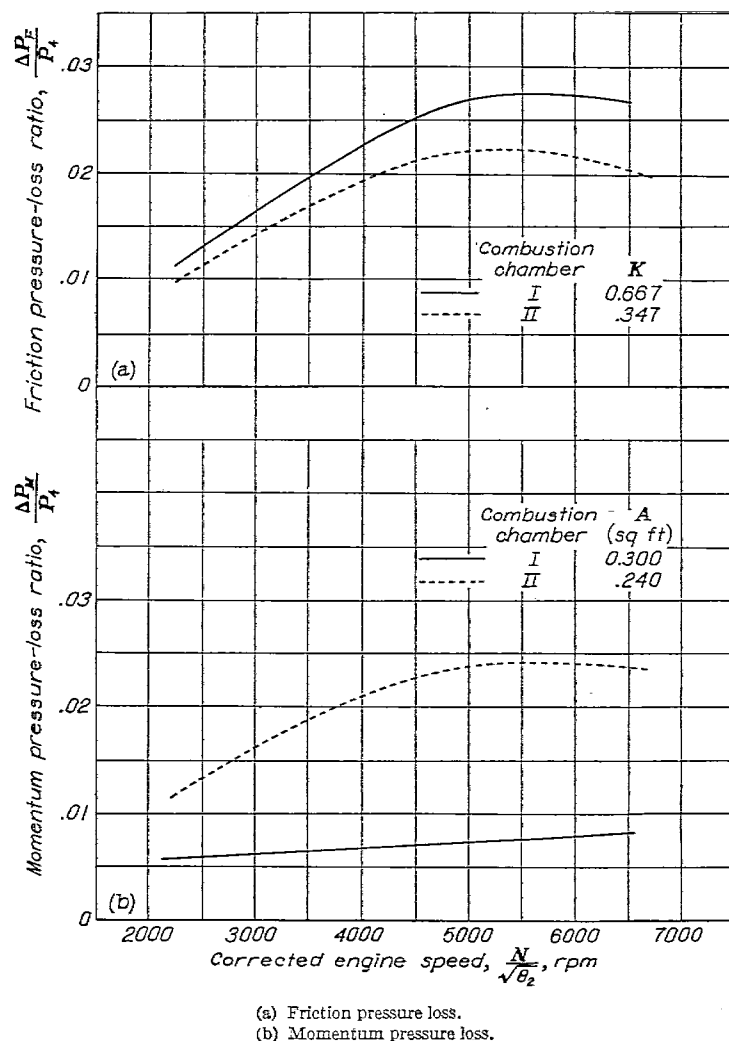


FIGURE 7.—Comparison of computed friction and momentum pressure-loss ratios for two types of combustion chamber.

combustion chamber for a ram jet are given in tables I and II, respectively. The data for the annular combustion chamber were obtained with the combustion chamber directly connected to an air source of variable temperature and an exhaust system capable of reproducing altitude pressures. The data for the combustion chamber of a ram jet were taken from tests of a complete 20-inch ram jet operating in the

TABLE I.—COMPARISON OF EXPERIMENTAL AND COMPUTED PRESSURE-LOSS RATIOS IN ANNULAR COMBUSTION CHAMBER

[$K=0.0132$ for entire combustion chamber; $A=1.58$ sq ft for entire combustion chamber; $KA^2=0.0330$ for entire combustion chamber or one-fourth segment]

$\frac{W\sqrt{T_4}}{P_4}$ (a)	$\frac{T_4}{T_1}$	Total pressure-loss ratio $\frac{\Delta P_T}{P_4}$		Difference (percent)
		Computed	Experimental	
0.0339	2.93	0.0243	0.0229	6.1
.0393	2.73	.0315	.0315	0
.0451	2.02	.0335	.0317	5.7
.0480	2.60	.0459	.0430	6.7
.0497	2.49	.0484	.0478	1.3

* These values were computed by using a one-fourth segment of the combustion chamber; that is, values of $W\sqrt{T_4}/P_4$ used on the chart are one-fourth the value for the entire combustion chamber.

Cleveland altitude wind tunnel. For both combustion chambers, the pressure-loss ratios computed from the chart are within 7 percent of the experimental values.

Significance of K and A .—The concept of the equivalent combustion chamber of constant cross section can serve as a convenient basis for comparing the pressure-loss characteristics of combustion chambers of a variety of designs. The values of KA_c^2 and A/A_c , where A_c is the maximum area of cross section of the combustion chamber, can be taken as figures of merit along with other criteria for comparing the excellence of combustion chambers. Good combustion chambers should have low values of KA_c^2 and high values of A/A_c .

The values of K and A obtained from the pressure-loss chart indicate how a combustion chamber should be modified to reduce the pressure losses. If pressure losses are high because of large values of K , improvement is obtained by opening the air-flow passages, particularly in the basket. If pressure losses are high because of low values of A , improvement is obtained by devoting more of the combustion-chamber cross section to the combustion zone. The combustion-chamber pressure losses can also be reduced by

TABLE II.—COMPARISON OF EXPERIMENTAL AND COMPUTED PRESSURE-LOSS RATIOS IN A RAM-JET COMBUSTION CHAMBER

[$K=0.00364$ for entire combustion chamber; $A=2.16$ sq ft for entire combustion chamber; $KA^2=0.0170$ for entire combustion chamber or 60° segment; actual area of combustion chamber, 2.18 sq ft]

Altitude (ft)	$\frac{W\sqrt{T_4}}{P_4}$ (a)	$\frac{T_4}{T_1}$	Total pressure-loss ratio $\frac{\Delta P_T}{P_4}$		Difference (percent)
			Computed	Experimental	
6,000	0.0303	2.14	0.0133	0.0127	4.7
6,000	.0593	2.39	.0595	.0583	6.6
10,000	.0341	2.36	.0179	.0180	-.0
10,000	.0543	2.39	.0492	.0450	2.5
10,000	.0708	1.33	.0463	.0458	1.1
15,000	.0359	3.77	.0276	.0230	-4.8
15,000	.0393	1.92	.0198	.0186	6.4
15,000	.0547	1.68	.0345	.0327	5.5

* These values are for a 60° segment of the combustion chamber.

altering the relative proportions of primary and secondary air and the manner of induction of the air into the combustion zone.

The assumption that the value of A for a given combustion chamber is fixed for all conditions of engine operation applies only if the flame is always seated at the same location in the combustion zone. Preliminary evidence shows that, for some combustion chambers, the value of A decreases with values of $W\sqrt{T_4}/P_4$ above a critical value, which is characteristic of the combustion chamber. This decrease in the value of A is believed to be associated with the movement of the flame seat or the zone of maximum combustion rate downstream. If this supposition is correct, a rapid rate of decrease of A with increasing values of $W\sqrt{T_4}/P_4$ may serve as an indication that blow-out conditions in the combustion chamber are being approached.

AIRCRAFT ENGINE RESEARCH LABORATORY,
NATIONAL ADVISORY COMMITTEE FOR AERONAUTICS,
CLEVELAND, OHIO, July 31, 1946.

APPENDIX

DEVELOPMENT OF EXPRESSION FOR MOMENTUM PRESSURE LOSS

The momentum pressure loss in a chamber of constant cross section, neglecting friction, is developed. A similar development is given in reference 1 for the static-pressure drop accompanying the addition of heat to a flowing gas. The expression is required in terms of the loss in total pressure.

The drop in static pressure required to accelerate the gas flow at any section in the combustion chamber is

$$dp = -\frac{\rho v}{g} dv \quad (9)$$

For steady flow in a combustion chamber of constant cross section

$$W = \rho A v$$

or

$$\rho v = C \quad (10)$$

where C is a constant. From equations (9) and (10)

$$\int_{p_B}^{p_s} dp = -\frac{C}{g} \int_{v_B}^{v_s} dv$$

$$p_s - p_B = \frac{\rho_B v_B^2 - \rho_s v_s^2}{g} \quad (11)$$

where $p_s - p_B$ is the static-pressure drop across the combustion zone. From the relations

$$M^2 = \frac{v^2}{\gamma g R t}$$

and

$$\frac{p}{\rho} = R t$$

combined to give

$$\rho \frac{v^2}{g} = \gamma p M^2$$

equation (11) can be written

$$p_s - p_B = \gamma_B p_B M_B^2 - \gamma_s p_s M_s^2 \quad (12)$$

or

$$p_s(1 + \gamma_s M_s^2) = p_B(1 + \gamma_B M_B^2)$$

$$\frac{p_s}{p_B} = \frac{1 + \gamma_B M_B^2}{1 + \gamma_s M_s^2} \quad (13)$$

From the relation between static pressure and total pressure

$$\frac{P}{p} = \left(1 + \frac{\gamma - 1}{2} M^2\right)^{\frac{\gamma}{\gamma - 1}}$$

equation (13) takes the form

$$\frac{P_s}{P_B} = \frac{(1 + \gamma_B M_B^2) \left(1 + \frac{\gamma_s - 1}{2} M_s^2\right)^{\frac{\gamma_s}{\gamma_s - 1}}}{(1 + \gamma_s M_s^2) \left(1 + \frac{\gamma_B - 1}{2} M_B^2\right)^{\frac{\gamma_B}{\gamma_B - 1}}} \quad (14)$$

or

$$1 - \frac{P_s}{P_B} = \frac{P_B - P_s}{P_B} = \frac{\Delta P_M}{P_B} = 1 - \frac{(1 + \gamma_B M_B^2) \left(1 + \frac{\gamma_s - 1}{2} M_s^2\right)^{\frac{\gamma_s}{\gamma_s - 1}}}{(1 + \gamma_s M_s^2) \left(1 + \frac{\gamma_B - 1}{2} M_B^2\right)^{\frac{\gamma_B}{\gamma_B - 1}}}$$

which is the desired equation and is equation (6) of the text.

REFERENCE

1. Bailey, Neil P.: The Thermodynamics of Air at High Velocities. Jour. Aero. Sci., vol. 11, no. 3, July 1944, pp. 227-238.